Non-Gaussian behavior of the displacement statistics of interacting colloidal particles

A. van Veluwen and H. N. W. Lekkerkerker
Van 't Hoff Laboratory, University of Utrecht, Padualaan 8, 3584 CH Utrecht, The Netherlands
(Received 21 December 1987)

A colloidal dispersion consisting of optically matched host particles and a small amount of strongly scattering tracer particles has been studied with dynamic light scattering. Analysis of the self-dynamic structure factor $F_s(q,t)$ obtained from these measurements demonstrates that the displacement statistics of the interacting colloidal particles shows considerable non-Gaussian behavior.

I. INTRODUCTION

In recent years a considerable interest has arisen in the Brownian motion of interacting colloidal particles.[1,2] In concentrated dispersions, the Brownian motion of a colloidal particle is influenced by direct interactions and hydrodynamic interactions with other particles. The Brownian motion of a given particle depends, therefore, on the spatial configuration of the surrounding particles. This configuration will change significantly on a time scale τ_I, which is on the order of the time it takes for a particle to diffuse over its own diameter.[3] The effect of this change of the spatial configuration is that for times $\tau \cong \tau_I$ the mean-square particle displacement is no longer linear in time and the statistics of the particle displacement is expected to show non-Gaussian behavior.[3-6]

In this paper we report for the first time experimental results for the non-Gaussian behavior of the particle displacement statistics. By carrying out dynamic light scattering (DLS) experiments on colloidal dispersions consisting of optically matched host particles to which a small amount of strongly scattering tracer particles were added, we were able to measure the self-dynamic structure factor. Moreover, because the particles had a radius of 80 nm, we could follow the motions of the particles on the above-mentioned time scale τ_I.

In Sec. II we show how the self-dynamic structure factor of interacting colloidal particles can be obtained by DLS, and how the particle displacement statistics can be derived from it. Experimental details of the sample preparation and the light scattering method are described in Sec. III. In Sec. IV we present the results of the DLS measurements and determine the non-Gaussian statistics of the particle displacement. In Sec. V we discuss the conclusions that can be drawn from the present work.

II. THEORY

A. The self-dynamic structure factor

In a homodyne dynamic light scattering experiment one measures the normalized autocorrelation function of the scattered intensity

$$g^{(2)}(t)=\frac{\langle I(0)I(t)\rangle}{\langle I\rangle^2}=\frac{\langle E(q,0)E^*(q,0)E(q,t)E^*(q,t)\rangle}{\langle I\rangle^2} . \quad (1)$$

Here $E(q,t)$ is the scattered electric field amplitude at scattering vector $q=(4\pi n/\lambda_0)\sin(\theta/2)$, where λ_0 is the wavelength of the light *in vacuo*, n is the refractive index of the suspension, and θ is the scattering angle. Since the scattered light will have Gaussian statistics one has the (Siegert) relation[7]

$$g^{(2)}(t)=1+C\,|\,g^{(1)}(t)\,|^2 , \quad (2)$$

where $C(0<C\leq 1)$ is a constant which is determined by experimental factors such as the optical detection configuration and $g^{(1)}(t)$ is the normalized autocorrelation function of the scattered electric field amplitude

$$g^{(1)}(t)=\frac{\langle E(q,0)E^*(q,t)\rangle}{\langle I\rangle}=\frac{F^M(q,t)}{S^M(q)} . \quad (3)$$

Here $F^M(q,t)$ is the measured dynamic structure factor and $S^M(q)=F^M(q,0)$ is the measured static structure factor.

For N rigid spherical particles, the measured dynamic structure factor is given by[2]

$$F^M(q,t)=[N\overline{f^2(q)}]^{-1}\times\sum_{i,j=1}^{N}\langle f_i(q)f_j(q)\exp\{i\mathbf{q}\cdot[\mathbf{r}_i(0)-\mathbf{r}_j(t)]\}\rangle , \quad (4)$$

where $f_j(q)$ is the scattering amplitude of particle j, and $r_j(t)$ is its position at time t.

In the Rayleigh-Gans-Debye approximation[8] the scattering amplitude of a homogeneous spherical particle with refractive index n_j can be written as

$$f_j(q)=V_j(n_j-n_0)B(q) , \quad (5)$$

where V_j is the volume of the particle, n_0 is the refractive index of the dispersion medium, and $B(q)$ is the square root of the form factor $P(q)\equiv B^2(q)$. If the particles are identical in terms of size and interactions but differ in scattering power, i.e., refractive index, then Eq. (4) can be

written rigorously in terms of ensemble averages and number averages. The number averages are given by

$$\overline{f^m} \equiv N^{-1} \sum_{i=1}^{N} f_i^m \tag{6}$$

and Eq. (4) reduces to[1]

$$F^M(q,t) = (\bar{f}^2/\overline{f^2})F(q,t) + (1-\bar{f}^2/\overline{f^2})F_s(q,t) , \tag{7}$$

where

$$F(q,t) = N^{-1} \sum_{i,j=1}^{N} \langle \exp\{i\mathbf{q}\cdot[\mathbf{r}_i(0)-\mathbf{r}_j(t)]\} \rangle \tag{8}$$

is the full dynamic structure factor and

$$F_s(q,t) = \langle \exp\{i\mathbf{q}\cdot[\mathbf{r}(0)-\mathbf{r}(t)]\} \rangle \tag{9}$$

is the self-dynamic structure factor. The first and second term in Eq. (7) are also described as the "coherent" and "incoherent" parts of F^M.

Under a refractive index matching condition, i.e.,

$$n_0 = \bar{n} \equiv N^{-1} \sum_{i=1}^{N} n_i , \tag{10}$$

we see that

$$\bar{f} = VB(q)(\bar{n} - n_0) = 0$$

and so the measured structure factor is identical to F_s. Away from the match point, n_0 differs from the number averaged refractive index of the particles. In such a case one measures both F_s and F. Because $F(q,0) = S^I(q)$ is the structure factor of the (ideal) monodisperse suspension, the ratio of the coherent to the incoherent (self) part of F^M is given by

$$\frac{A_c}{A_s} = \frac{\bar{f}^2 S^I(q)}{\overline{f^2} - \bar{f}^2} . \tag{11}$$

For a suspension that consists of two types of particles with refractive indices n_1 and n_2 at relative concentration α and $1-\alpha$, the refractive index-matching condition, Eq. (10), becomes

$$n_0 = \bar{n} = n_2 + \alpha(n_1 - n_2) , \tag{12}$$

and Eq. (11) becomes

$$\frac{A_c}{A_s} = \frac{(n_2 - n_0 + \alpha[n_1 - n_2])^2 S^I(q)}{\alpha(1-\alpha)[n_1 - n_2]^2} . \tag{13}$$

In practice, self-diffusion may be observed by performing a tracer experiment, i.e., adding a small amount ($\alpha \ll 1$) of strongly scattering tracer particles to a matched host dispersion ($n_2 = n_0$). The summation in Eq. (4) runs only over the N_1 tracer particles for which $f_i(q) \neq 0$, and if this number is sufficiently small ($N_1 \ll N$) cross terms $i \neq j$ may be neglected. However, the concept of a genuine tracer experiment is somewhat illusory because from Eq. (12) we see that the refractive index of the medium should be equal to the number averaged refractive index of the particles, which changes after the addition of the tracer particles. The question of how many tracer particles can be added before a significant amount of coherent scattering is observed is equivalent to the question of how far away from the match point one can operate. The answers to both questions can be found from Eq. (13), which for $n_2 = n_0$ and $\alpha \ll 1$ reduces to $A_c / A_s = \alpha S^I(q)$.

B. Statistics of the particle displacement

The self-dynamic structure factor is the spatial Fourier transform of the probability density function $P(\Delta\mathbf{r},t)$ for a particle to have undergone a displacement $\Delta\mathbf{r}$ in a time t,

$$F_s(q,t) = \int P(\Delta\mathbf{r},t) e^{i\mathbf{q}\cdot\Delta\mathbf{r}} d(\Delta\mathbf{r}) .$$

Because F_s is a moment generating function of P, a cumulant expansion[9] of $\ln F_s$ in powers of q gives

$$F_s(q,t) = \exp[-q^2\rho_1(t) + q^4\rho_2(t) - \cdots] , \tag{14}$$

where the ρ's are given by

$$\begin{aligned} \rho_1(t) &= \tfrac{1}{6}\langle \Delta r^2(t) \rangle , \\ \rho_2(t) &= \tfrac{1}{360}[3\langle \Delta r^4(t) \rangle - 5\langle \Delta r^2(t) \rangle^2] , \end{aligned} \tag{15}$$

etc. If the particle displacements have Gaussian statistics, i.e., the probability density function $P(\Delta\mathbf{r},t)$ has a Gaussian form, then all cumulants except $\rho_1(t)$ are zero. This means that the value of $\rho_2(t)$ provides a first measure of the non-Gaussian behavior.

Following Rahman,[10] the non-Gaussian behavior of $P(\Delta\mathbf{r},t)$ may be expressed in terms of the function $\alpha_2(t)$ defined as

$$\alpha_2(t) \equiv \frac{2\rho_2(t)}{(\rho_1(t))^2} = \frac{3\langle \Delta r^4(t) \rangle - 5\langle \Delta r^2(t) \rangle^2}{5\langle \Delta r^2(t) \rangle^2} . \tag{16}$$

For noninteracting particles, the displacement $\Delta\mathbf{r}$ is a Gaussian variable for times larger than the relaxation time $\tau_B = m/(6\pi\eta a)$ of the Brownian fluctuations in the particle velocities (m is the particle mass, a is its radius, and η is the viscosity of the solvent. The Brownian motion of independent spherical colloidal particles can be characterized by the single-particle diffusion coefficient

$$D_0 = \frac{kT}{6\pi\eta a} ,$$

where k is Boltzmann's constant and T is the absolute temperature. The mean-square displacement of a particle is linear in time for all times much larger than τ_B

$$\langle \Delta r^2(t) \rangle = 6D_0 t, \quad t \gg \tau_B . \tag{17}$$

For interacting particles, one has to take into account that for times larger than $\tau_1 \sim a^2/D_0$ the particle velocity ceases to be a stationary random function of time.[3] The mean-square displacement is now only linear for "short" times $\tau_B \ll t \ll \tau_I$ and "long" times $t \gg \tau_I$,

$$\langle \Delta r^2(t) \rangle = \begin{cases} 6D_s^{\text{short}} t, & \tau_B \ll t \ll \tau_I \\ 6D_s^{\text{long}} t, & t \gg \tau_I \end{cases} \tag{18}$$

where D_s^{short} and D_s^{long} are the short- and long-time self-diffusion coefficients, respectively. In addition, the particle displacement is no longer expected to be a Gaussian variable at time scales comparable to τ_I.[3-6]

III. EXPERIMENT

The host particles in the dispersions studied consisted of silica cores sterically stabilized with poly(isobutylene) (PIB).[11] The tracer particles were poly(methylmethacrylate) (PMMA) particles sterically stabilized by poly(12-hydroxy stearic acid) (PHS).[12] The particle radii were determined by DLS in dilute suspensions. Both types of particles have a radius a of 80 ± 1 nm. The relative standard deviations in size are approximately $\sigma=10\%$ for the silica particles and $\sigma=15\%$ for the PMMA particles.

For particles of this size, qa is of order unity. Since the self-dynamic structure factor decays essentially as $\exp[-q^2\langle\Delta r^2(t)\rangle/6]$, we thus are able to measure motions both at "short" times, i.e., times for which $\langle\Delta r^2(t)\rangle^{1/2}<a$, as well as at "long" times, i.e., times for which $\langle\Delta r^2(t)\rangle^{1/2}>a$.

To perform a tracer experiment, one has to select a solvent with a refractive index close to that of the host particles. Both types of particles have to form stable dispersions in this solvent. Furthermore, mixtures of these dispersions have to remain stable too. This last condition is often the most difficult to achieve. We found that cyclo-octane satisfies all these requirements. Mixtures of the silica and the latex particles in this solvent show no sign of phase separation or aggregation. At 41 °C the host particles are optically matched in cyclo-octane for the 632-nm He-Ne laser line. The scattered intensities of these silica particles showed a broad minimum around this temperature. This indicates that the host dispersion is already optically polydisperse in itself. However, the residual (incoherent) scattered intensity in the match-point is too low to obtain intensity autocorrelation functions of sufficient accuracy for further quantitative analysis. Therefore a small amount of tracer particles has to be added. The difference between the refractive indices of the latex and the silica particles, $n_1-n_2\approx0.05$, is large enough to ensure that even a small amount of tracer particles provides strong incoherent scattering.

Medium concentrated stock dispersions in cyclo-octane were made dust free by means of filtration through Millipore filters. The host dispersion was brought up to the required concentration by centrifugation and removal of the supernatant. The ultimate weight fraction was measured by drying weighed samples taken from the (cylindrical) measurement cell. Finally the tracer dispersion was obtained by adding a few drops of the medium-concentrated PMMA dispersion (of known weight fraction) to this host dispersion. Volume fractions ϕ were calculated from the weight fractions using the densities of the silica particles, PMMA particles and solvent, 1.60, 1.19, and 0.834 g/cm^3, respectively.

The He-Ne laser beam was focused in the sample cell, which was placed in a cylindrical refractive index matching bath. The temperature of this surrounding bath was controlled within 0.1 °C. Autocorrelation functions were measured with a Malvern Multibit K7025 128-channel correlator at a number of angles between 30° and 150°, all with the same sample time of 20 μs. In order to measure D_s^{long} in concentrated dispersions, additional measurements were made with much longer sample times at small scattering angles.

IV. RESULTS AND DISCUSSION

A. Measurement of the self-dynamic structure factor

The maximum value of qa reached in the experiments was less than 2.3. For a hard-sphere system this means that $S(q)\leq1$. If we require the ratio of coherent to incoherent scattering to be less than 1%, then, from Eq. (13), we see that the fraction α of tracer particles should be less than 0.01. Owing to the optical polydispersity of the host dispersion, this requirement is actually less stringent because the calculation really applies to the case of pure monodisperse host particles.

The influence of the (number of) tracer particles was determined by comparing DLS measurements on a dispersion of volume fraction $\phi=0.145$ before and after the addition of the tracer particles at relative concentration $\alpha=0.01$. In order to estimate the influence of the refractive index of the solvent, these autocorrelation functions were measured at a number of temperatures and their decay rates were compared, after correction for the temperature dependency of D_0.

At all angles and temperatures with the exception of the match point, the decay of the measured intensity autocorrelation function was slower after the addition of the tracer particles, clear evidence of the presence of the slowly decaying self-dynamic structure factor. For the tracer dispersion, the temperature-corrected decay rate was relatively insensitive to temperature in a range of ±5 °C around the match point (40 °C). Far away from the match point the coherent scattering begins to dominate, especially for the host dispersion. The (initial) decay rate of the full dynamic structure factor decreases with increasing scattering angle, but this decay is always faster than the decay rate of the self-dynamic structure factor.

Increasing the number of tracer particles from $\alpha=0.01$ to $\alpha=0.02$ only led to an increase of the scattered intensity, and thereby to a better signal-to-noise ratio, but showed little or no further effect on the measured dynamic structure factors. We concluded that at 41 °C the influence of coherent scattering could be completely neglected for the tracer system. In any case, the unwanted contribution of coherent scattering would be maximal at the highest angles (q values) where $S(q)$ is largest, and this would lead to the introduction of a rapidly decaying mode at those high-q values. As will be discussed in Sec. IV B an opposite effect is observed, which can be fully attributed to the non-Gaussian terms in the self-dynamic structure factor. To achieve a reasonable signal-to-noise ratio without danger of multiple scattering, only the lowest two concentrations were prepared with a relative fraction of tracer particles $\alpha=0.02$, whereas the other concentrations were prepared with $\alpha=0.01$.

B. Analysis of the self-dynamic structure factor

All measurements of the intensity autocorrelation function from which the self-dynamic structure factor was obtained were made at 41 °C. By definition, $g^{(1)}(0)=1$, and therefore, according to Eq. (2), $g^{(2)}(0)=1+C$. This means that the experimental factor C can be obtained by extrapolating the measured values of $g^{(2)}(t)$ for very small times [i.e., times for which $g^{(2)}(t)$ has hardly decayed from its initial value] to $g^{(2)}(0)$. Having thus determined the factor C, the normalized field autocorrelation function $g_1=F_s$ was obtained by taking the square root of $[g^{(2)}(t)-1]/C$.

In Fig. 1 we present $-\ln F_s(q,t)/(q^2a^2)$ as a function of delay time t for various scattering angles. The volume fraction ϕ of the particles in the sample was 0.31 and the relative concentration of tracer particles to host particles was 0.01. From Eqs. (14) and (15) it follows that when the particle displacements due to Brownian motion have statistics of Gaussian form, the function $-\ln F_s(q,t)/(q^2a^2)$ for different scattering angles (which correspond to different values of the scattering vector q) should coincide. Indeed we found that in an infinitely dilute suspension, plots of $-\ln F/q^2$ did coincide. This is a clear indication that the noncoincidence of the curves in Fig. 1 has not been caused by polydispersity of the tracer particles, or even by a possible misalignment of the optical system. The fact that the curves do not coincide indicates that $P(\Delta\mathbf{r},t)$ departs from a Gaussian. In order to extract the first non-Gaussian term we plot $-\ln F_s(q,t)/(q^2a^2)$ as a function of q^2 for various values of t (Fig. 2). We can extract the mean-square displacement $\langle\Delta r^2(t)\rangle$ from the intercept at $q=0$, and $[3\langle\Delta r^4(t)\rangle-5\langle\Delta r^2(t)\rangle^2]$ from the slope. From this we calculated $\alpha_2(t)$ according to Eq. (16).

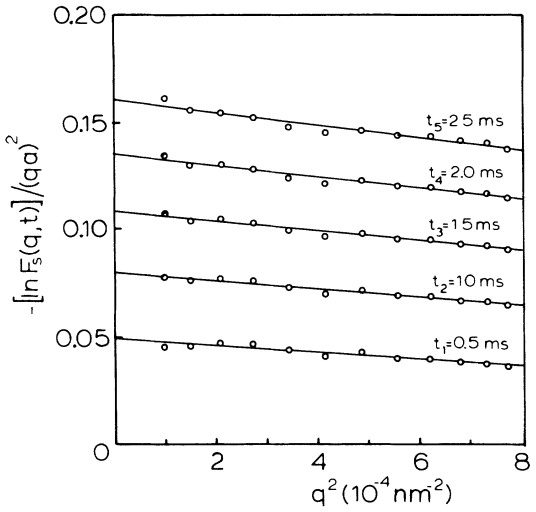

FIG. 2. Plot of $-\ln F_s(q,t)/(qa)^2$ as a function of the square of the scattering vector q for volume fraction $\phi=0.31$ at delay times t_1 to t_5 as indicated in Fig. 1. Solid lines are linear fits.

In Fig. 3 we plot the mean-square displacement as obtained from this extrapolation procedure. From the initial and final slopes of the mean-square displacement, we obtain the short-time self-diffusion coefficient D_s^{short} and the long-time self-diffusion coefficient D_s^{long}. The final slope of $\langle\Delta r^2(t)\rangle$ of the highest concentrations is not visible in Fig. 3. As discussed in Sec. III, this final slope was obtained from DLS measurements over a longer time span. The self-diffusion coefficients for various values of the volume fractions ϕ of the dispersed particles, shown in Fig. 4, are in agreement with results reported by

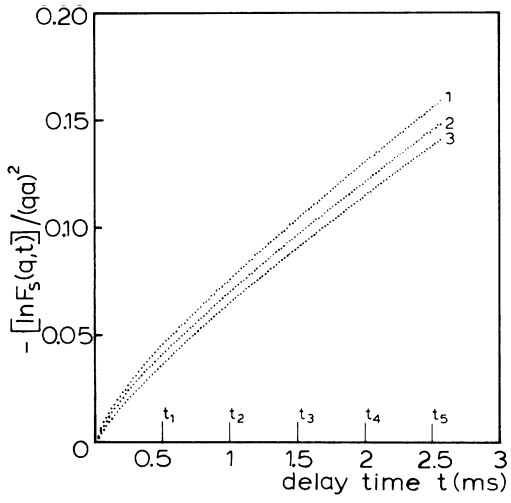

FIG. 1. Logarithm of the self-dynamic structure factor F_s, divided by $(qa)^2$, vs delay time t for volume fraction $\phi=0.31$ at three different scattering angles: (1) $\theta=50°$, $q=1.21\times10^{-2}$ nm^{-1}, (2) $\theta=90°$, $q=2.03\times10^{-2}$ nm^{-1}, and (3) $\theta=150°$, $q=2.78\times10^{-2}$ nm^{-1}. The times at which $-\ln F_s/(qa)^2$ is plotted as a function of q^2 (Fig. 2) are indicated on the abscissa.

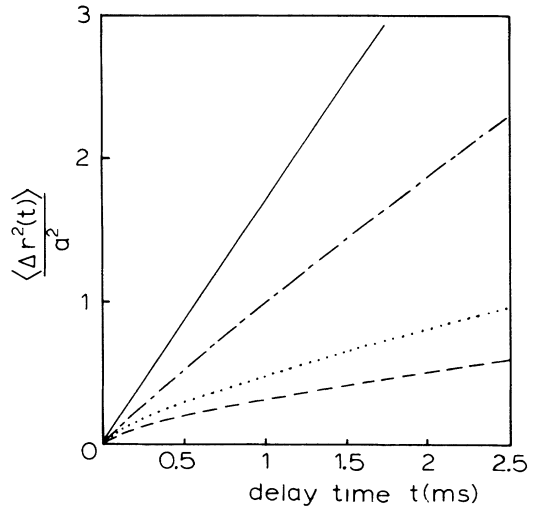

FIG. 3. Mean-square displacement vs delay time t, showing free diffusion (——) and results for volume fractions $\phi=0.14_5$ (—·—·), $\phi=0.31$ (· · · ·), and $\phi=0.37$ (— — —).

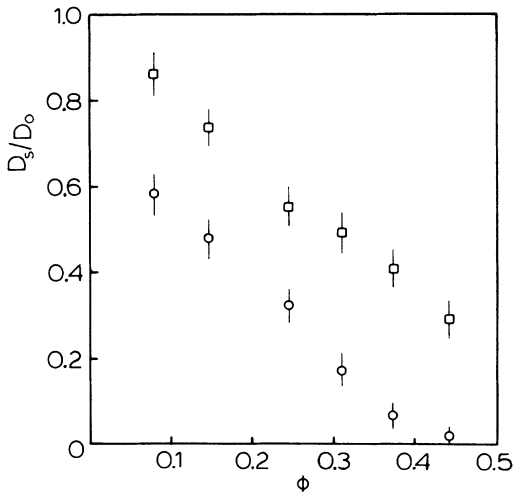

FIG. 4. Normalized self-diffusion coefficients D_s/D_0 as a function of volume fraction ϕ: short-time self-diffusion D_s^{short}/D_0 (□) and long-time self-diffusion D_s^{long}/D_0(○).

Ottewill and Williams.[13] The experimentally observed strong decrease of the long-time self-diffusion for the hard sphere dispersions studied here differs considerably from the theoretically predicted behavior of high charged colloidal particles with a soft long range repulsion.[14] Apparently the long-time self-diffusion coefficients are very sensitive functions of the steepness of the repulsive interaction between the particles.

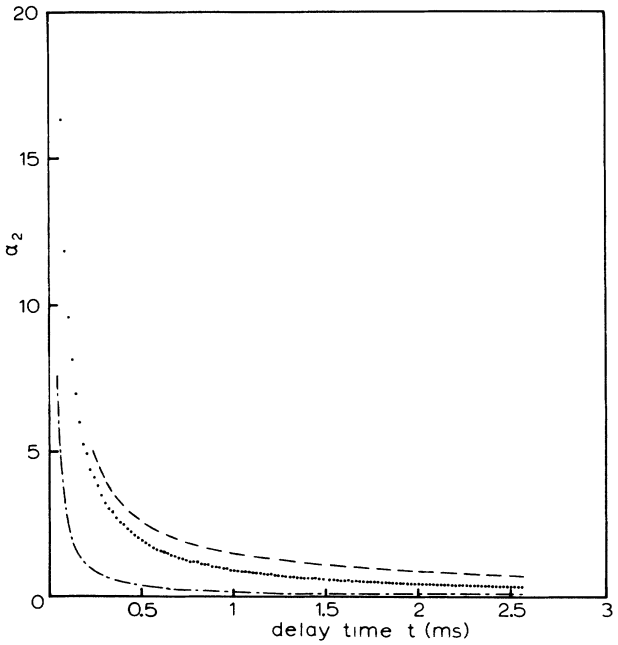

FIG. 5. Non-Gaussian behavior of F_s expressed as α_2 vs t, showing the results for volume fractions $\phi=0.14_5$ (– – – –), $\phi=0.31$ (· · · ·), and $\phi=0.37$ (— — —).

In Fig. 5 we plot $\alpha_2(t)$ as a function of t for different volume fractions ϕ. Like in the case of the molecular-dynamics simulation of liquid argon by Rahman,[10] we find that $\alpha_2(t)$ is positive. The measurement errors in α_2, as calculated from the fitting procedure, are 10–20%, a range which is comparable with the reproducibility of the measurements. These estimates do not include possible systematic errors. For example, such an error might be introduced by the rescaling of the autocorrelation functions. Incorrect rescaling, such that $F_s(q,0)\neq 1$, might lead to an absolute systematic error in ρ_1. The influence of this error on α_2 would be largest at the shortest times, where $\rho_1\approx 0$. Because of these considerations, we did not plot in Fig. 5 the values of α_2 obtained at the shortest times.

V. CONCLUDING REMARKS

We have found experimental evidence for the occurrence of large non-Gaussian effects in the displacement statistics of tracer particles in concentrated dispersions. In view of the delicate manipulations required to derive these effects from the data, we paid close attention to possible experimental artifacts. We are confident that our results are not caused by polydispersity of the tracer particles, or possible alignment errors in the optical system, multiple scattering and/or a contribution of coherent scattering. The fact that non-Gaussian behavior was not observed in previous work[15] on colloidal tracer systems might be because in that case qa was much larger than 1, which restricts the measurements to short times.

We would like to point out that it cannot be concluded from our data that $\alpha_2(t)$ will diverge at short times, although the values of $\alpha_2(t)$ presented here roughly behave as t^{-1} on the time span observed. In order to establish the behavior of $\alpha_2(t)$ at very short times experiments have to be done using particles with a radius larger than 80 nm r.

We found that $\alpha_2(t)$ is positive, which means that the probability density function $P(\Delta\mathbf{r},t)$ for the particle displacements $\Delta\mathbf{r}$ in a time t has a higher central peak and broader skirts than a Gaussian function of the same standard deviation. From this it follows that both very small and very large values of the displacement are more probable than for a normal distribution of the same standard deviation.[16] A significant quantitative difference of the present experimental results for the Brownian movement of colloidal particles with the molecular-dynamics simulation results for liquid argon is that the value of $\alpha_2(t)$ obtained here is roughly one order of magnitude larger and appears to decay to zero much slower. Gaylor *et al.*[4] performed Brownian dynamics simulations for a dilute dispersion of particles interacting with a long-ranged weakly screened Coulomb pair potential and obtained results for $\alpha_2(t)$ comparable to those obtained by Rahman in his molecular-dynamics simulation of liquid argon. So

far no Brownian dynamics simulations of concentrated hard-sphere dispersions have been reported. In light of our new and unexpected experimental results, it would be extremely interesting to perform such calculations to see whether they would provide further evidence for the pronounced non-Gaussian behavior of the particle displacement statistics observed in the present study.

The significant difference of the behavior of the non-Gaussian term with the corresponding quantity for simple liquids indicates that notwithstanding some formal similarities between the dynamics of concentrated particle dispersions and simple liquids there are apparently also important differences.

ACKNOWLEDGMENTS

The silica and latex particles used in this study were synthesized by Mr. C. Slob and Mr. C. Pathmamanoharan. We are grateful to them for providing these systems to us. Mr. S. Coenen is thanked for assistance with the DLS measurements. We thank Dr. C. G. de Kruif, Dr. W. van Megen, Dr. P. N. Pusey, and Professor A. Vrij for a number of valuable discussions concerning this work. This work is part of the research program of the Foundation for Fundamental Research of Matter (FOM) with financial support from the Netherlands Organization for Pure Research (ZWO).

[1]P. N. Pusey and R. J. A. Tough, *Dynamic Light Scattering: Applications of Photon Correlation Spectroscopy,* edited by R. Pecora (Plenum, New York, 1985), p. 85.

[2]W. Hess and R. Klein, Adv. Phys. **32**, 173 (1983).

[3]J. M. Rallison and E. J. Hinch, J. Fluid Mech. **167**, 131 (1986).

[4]K. Gaylor, I. Snook, and W. van Megen, J. Chem. Phys. **75**, 1682 (1981).

[5]P. N. Pusey and R. J. A. Tough, Faraday Discuss. Chem. Soc. **76**, 123 (1983).

[6]R. J. A. Tough, P. N. Pusey, H. N. W. Lekkerkerker, and C. van den Broeck, Mol. Phys. **59**, 595 (1986).

[7]H. Z. Cummins and H. L. Swinney, *Progress in Optics,* edited by E. Wolf (North-Holland, Amsterdam, 1970), Vol. VIII, p. 133.

[8]M. Kerker, *The Scattering of Light* (Academic, New York, 1969).

[9]N. G. van Kampen, *Stochastic Processes in Physics and Chemistry* (North-Holland, Amsterdam, 1982), p. 6.

[10]A. Rahman, Phys. Rev. **136**, A405 (1964).

[11]C. Pathmamanoharan (unpublished).

[12]L. Antl, J. W. Goodwin, R. D. Hill, R. H. Ottewill, S. M. Owens, S. Papworth, and J. A. Waters, Colloid Surf. **17**, 67 (1986).

[13]R. H. Ottewill and N. St. J. Williams, Nature **325**, 232 (1987).

[14]G. Nägle, M. Medina-Noyola, J. L. Auraz-Lara, and R. Klein, Progr. Colloid Polymer Sci. **73**, 5 (1987).

[15]W. van Megen, S. M. Underwood, and I. Snook, J. Chem. Phys. **85**, 4065 (1986).

[16]G. K. Batchelor, *The Theory of Homogeneous Turbulence* (Cambridge University Press, Cambridge, 1953), p. 184.